American Mineralogist, Volume 63, pages 87–95, 1978

Calculation of metamorphic pressure using the sphalerite–pyrrhotite–pyrite equilibrium

IAN HUTCHEON[1]

Geology Department, Carleton University
Ottawa, Ontario, Canada K1S 5 B6

Abstract

The activity coefficients of FeS and ZnS in sphalerite in the temperature range 580 to 850°C can be expressed in terms of a two-constant Margules solution model. The standard state of FeS in sphalerite is chosen as pure FeS with the sphalerite structure, rather than FeS with the structure of pyrrhotite. The fit parameters of an ordinary least-squares regression indicate that the activity of FeS and ZnS in sphalerite can be adequately represented by a solution model in which the activity is independent of temperature. The excess partial molar free energy at infinite dilution is given by:

$$\bar{G}^{ex}_{ZnS} = 0.642\ T$$

$$\bar{G}^{ex}_{FeS} = 1.158\ T$$

The solution model can be extrapolated to lower temperatures and will accurately predict the composition of sphalerite in sphalerite–pyrrhotite experiments. If a^{po}_{FeS} is allowed to be constant below 525°C the matrix compositions of sphalerite from published sphalerite–pyrrhotite–pyrite experiments can be reproduced. If a^{po}_{FeS} is allowed to vary with temperature below 525°C the solution model predicts sphalerite compositions between the composition of the matrix and iron-rich patches in published experiments.

The *P–T–X* relations of sphalerite–pyrrhotite–pyrite assemblages can be calculated using published data for the pyrite–pyrrhotite equilibrium and molar volumes and activities from the sphalerite solution model. Calculated isobars are in agreement with published experiments at elevated pressures.

Application of the calculated isobars to sphalerite compositions from the Stall Lake Mine, near Snow Lake, Manitoba, indicates the total pressure of metamorphism was 7 ± 1.0 kbar.

Introduction

Kullerud (1953) recognized the potential of the FeS content of sphalerite as an indicator of the conditions of sulfide deposition. Barton and Toulmin (1966), Boorman (1967), Scott and Barnes (1971), and Scott (1973) have investigated the equilibrium among pyrite, hexagonal pyrrhotite, and sphalerite at various temperatures and pressures. Einaudi (1968) calculated the sphalerite–pyrrhotite–pyrite solvus at one bar from the data of Barton and Toulmin (1966). Scott (1973) has proposed that in the range from 300 to 600°C and pressures up to 5 kbar, the mole fraction of FeS in sphalerite is independent of temperature. Scott's geobarometer has seen widespread use as an indicator of the total pressure of metamorphism of sulfide orebodies (Bristol, 1974; Lusk *et al.*, 1975; Scott, 1976).

In this study the data of Barton and Toulmin (1966, Table 3) have been used to calculate the activity coefficients of FeS and ZnS in sphalerite by applying a two-constant Margules (sub-regular) solution model. These activity coefficients are combined with molar volume data and the pyrite–pyrrhotite equilibrium to calculate the phase relations of the assemblage sphalerite–pyrrhotite–pyrite over a range of temperatures and pressures. The calculated phase relations can be compared to experimental calibrations and used to estimate metamorphic conditions in pelitic rocks from the Stall Lake mine, near Snow Lake, Manitoba.

[1] Present address: Geology Department, The University of Calgary, Calgary, Alberta, Canada T2N 1N4.

0003-004X/78/0102-0087$02.00

From mineral zones in pelitic rocks, Froese and Gasparrini (1975) estimate 5.5 kbar pressure near Stall Lake. Scott (1976) estimates a pressure of 7 ± 0.9 kbar. An adequate estimate of the metamorphic pressure is necessary for a detailed study of the conditions of silicate–sulfide metamorphism in the Stall Lake mine.

Determination of activity coefficients for FeS and ZnS in sphalerite

Standard state

In this paper the standard state of FeS is defined as follows:

(1) For sphalerite the standard state of FeS is pure FeS, with the structure of sphalerite, at one atmosphere.

(2) For pyrrhotite the standard state of FeS is pure FeS, with the structure of pyrrhotite, at one atmosphere.

The chemical potential of FeS in sphalerite (μ^{sp}_{FeS}) is defined as follows:

$$\mu^{sp}_{FeS} = \mu^{*sp}_{FeS} + RT \ln\gamma^{sp}_{FeS} + RT \ln X^{sp}_{FeS}$$

and similarly for pyrrhotite:

$$\mu^{po}_{FeS} = \mu^{*po}_{FeS} + RT \ln\gamma^{po}_{FeS} + RT \ln X^{po}_{FeS}$$

where both sphalerite and pyrrhotite have the appropriate crystal structure and $\gamma \cdot X = a$ (activity). The unit activity state (μ^*) is defined so as to be consistent with Denbigh (1971, p. 270) for pyrrhotite and sphalerite, so that at unit concentration the activity is equal to unity at any pressure and temperature of interest. ΔG^0 refers to a standard state at one atmosphere. This choice of unit activity state is consistent with the observation that a component "i" of a real solution is normally found to approach ideal behavior, both as $X_i \to 0$ and $X_i \to 1$ (Denbigh, 1971).

For the equilibrium:

$$\text{FeS(pyrrhotite)} = \text{FeS(sphalerite)} \qquad (1)$$

$$K_{(1)} = a^{sp}_{FeS}/a^{po}_{FeS} \text{ and:}$$

$$G^0_{(1)} = -RT \ln K_{(1)} - \Delta V_s(P-1)$$

$$= -RT\,(\ln a^{sp}_{FeS} - \ln a^{po}_{FeS}) - \Delta V_s(P-1)$$

To obtain $\Delta G^0_{(1)}$ it is necessary to find values for a^{sp}_{FeS}. This may be done by expressing the variation of $\ln\gamma^{sp}_{FeS}$ and $\ln\gamma^{sp}_{ZnS}$ with composition, in terms of a power series, as derived by Carlson and Colburn (1942) from Margules (1895). By this method:

$$RT \ln\gamma^{sp}_{FeS} = (2\bar{G}^{ex}_{\infty ZnS} - \bar{G}^{ex}_{\infty FeS})\, X^{sp^2}_{ZnS} + 2(\bar{G}^{ex}_{\infty FeS} - \bar{G}^{ex}_{\infty ZnS})\, X^{sp^3}_{ZnS} \qquad (2)$$

$$RT \ln\gamma^{sp}_{ZnS} = (2\bar{G}^{ex}_{\infty FeS} - \bar{G}^{ex}_{\infty ZnS})\, X^{sp^2}_{FeS} + 2(\bar{G}^{ex}_{\infty ZnS} - \bar{G}^{ex}_{\infty FeS})\, X^{sp^3}_{FeS} \qquad (3)$$

where $\bar{G}^{ex}_{\infty FeS}$ and $\bar{G}^{ex}_{\infty ZnS}$ are the excess free energies of FeS and ZnS at infinite dilution.

The expressions for $RT \ln\gamma$ can be substituted into equilibrium (1) and an equation in three unknowns, $\Delta G^0_{(1)}$, $\bar{G}^{ex}_{\infty FeS}$ and $\bar{G}^{ex}_{\infty ZnS}$ is obtained. Assuming a linear temperature dependence of the unknowns:

$$\bar{G}^{ex}_{\infty FeS} = \bar{H}^{ex}_{\infty FeS} - T\bar{S}^{ex}_{\infty FeS}$$

$$\bar{G}^{ex}_{\infty ZnS} = \bar{H}^{ex}_{\infty ZnS} - T\bar{S}^{ex}_{\infty ZnS}$$

$$\Delta G^0_{(1)} = \Delta H^0 - T\Delta S^0$$

and each of the experimental determinations in Table 3 of Barton and Toulmin (1966) can be expressed as an equation in six unknowns. If $\ln\gamma$ is assumed to be independent of temperature then:

$$\bar{G}^{ex}_{\infty FeS} = -T\bar{S}^{ex}_{\infty FeS}$$

$$\bar{G}^{ex}_{\infty ZnS} = -T\bar{S}^{ex}_{\infty ZnS}$$

$$\Delta G^0_{(1)} = \Delta H^0 - T\Delta S^0.$$

and each experimental determination may then be expressed as an equation in four unknowns.

Data at 1104, 1001, 1000, and 925°C in Table 3 of Barton and Toulmin (1966) have been excluded because of the presence of wurtzite in some experimental runs. Data at 555°C were excluded because Barton and Toulmin report difficulty in obtaining equilibrium. Run 42A was also excluded because Scott and Barnes (1971) report it as aberrant. Each of the remaining 113 data points can be written as an equation in either six unknowns ($\ln\gamma$ is temperature dependent) or four unknowns ($\ln\gamma$ is independent of temperature). The 113 equations have been solved for both models, using ordinary least squares. The R^2 value, calculated for a least-squares fit with no constant term, for both the temperature dependent and independent models is 0.9976, indicating that 99.76 percent of the variation in the dependent variable ($RT \ln a^{po}_{FeS} - RT \ln X^{sp}_{FeS}$) can be explained by a model in which $\ln\gamma$ is not a function of temperature. The solution obtained for the temperature independent model is:

$$\bar{G}^{ex}_{\infty ZnS} = 0.642\ T$$

$$\bar{G}^{ex}_{\infty FeS} = 1.158\ T$$

$$\Delta G^0_{(1)} = 239 - 0.840\ T$$

Mixing properties of sphalerite solid solutions

Barton and Toulmin equate a^{po}_{FeS} with a^{sp}_{FeS}, choosing troilite as the standard state for FeS in sphalerite. Figure 1 shows μ^{sp}_{FeS} plotted against $\ln X^{sp}_{FeS}$. The value of μ^{*po}_{FeS}, plotted on Figure 1, shows that to apply a solution model in which the activity of a component is unity at unit concentration, the choice of standard state for FeS in sphalerite clearly cannot be troilite. The difference $\mu^{*sp}_{FeS} - \mu^{*po}_{FeS}$ is equal to $\Delta G^0_{(1)}$ ($\mu^* = \mu^0$ at one atmosphere). This difference can be used to convert the standard state for sphalerite in this paper to the standard state chosen by Barton and Toulmin (1966).

Fleet (1975) chose the same standard state as this study and graphically integrated the Gibbs-Duhem equation at 850°C using the data of Barton and Toulmin, accepting their assumption of non-temperature dependence of a^{sp}_{FeS}. Figure 2 shows the activities determined by Fleet compared to this study. There are minor differences in the ZnS-rich area, especially for a^{sp}_{ZnS}, but the difference between the activities over most of the compositional range is insignificant. The free energy of mixing

$$\Delta G^{mx} = X^{sp}_{FeS}\, RT \ln\gamma^{sp}_{FeS}\, X^{sp}_{FeS} + X^{sp}_{ZnS}\, RT \ln\gamma^{sp}_{ZnS}\, X^{sp}_{ZnS}$$

and the excess free energy of mixing

$$\Delta G^{ex} = X^{sp}_{ZnS}\, RT \ln\gamma^{sp}_{ZnS} + X^{sp}_{FeS}\, RT \ln\gamma^{sp}_{FeS}$$

are compared at 850°C and 1 atm to those determined by Fleet in Figure 3. The difference between

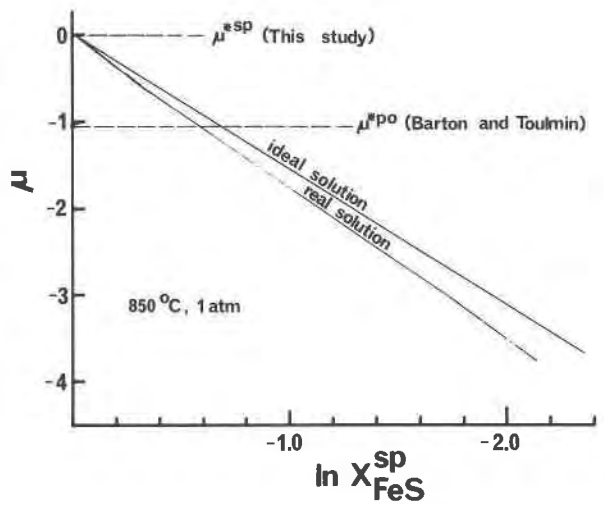

Fig. 1. The standard state of FeS in sphalerite is chosen so that the value of a^{sp}_{FeS} is unity for pure FeS sphalerite. The standard state chosen by Barton and Toulmin (1966) means that a^{sp}_{FeS} is not unity at unit concentration.

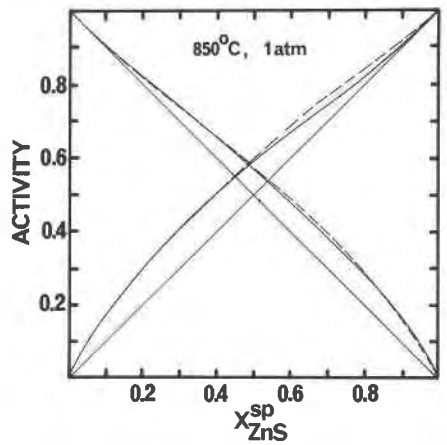

Fig. 2. A plot of activity *vs.* X^{sp}_{ZnS} at 850°C and 1 atm. Activities calculated by Fleet (1975) are shown by broken lines. Compositions from 0.0 to 0.45 X^{sp}_{ZnS} are metastable.

Fleet's values and those in this study is always less than 50 calories for a given sphalerite composition. The very slight differences between this study and Fleet's are probably related to the extrapolation of a smoothed curve for a^{po}_{FeS} *vs.* X^{sp}_{FeS} to perform the graphical integration.

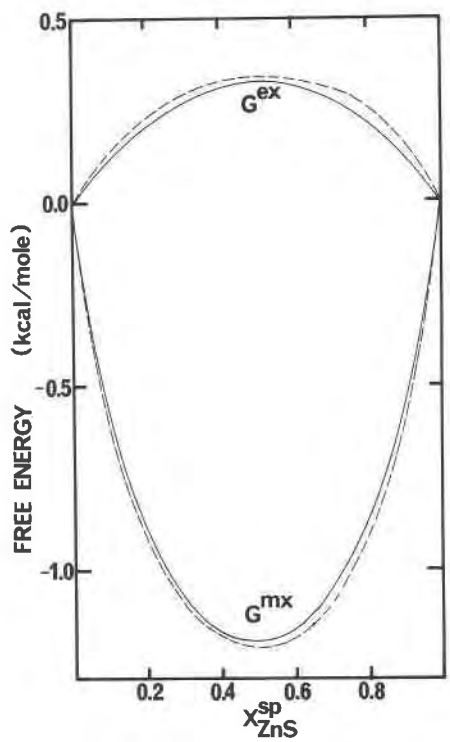

Fig. 3. Free energy *vs.* X^{sp}_{ZnS} at 850°C and 1 atm from this study (solid lines) compared to Fleet (broken lines). G^{ex} is the excess free energy of mixing, G^{mx} is the free energy of mixing. Compositions from 0.0 to 0.45 X^{sp}_{ZnS} are metastable.

Determination of pressure dependent activity coefficients and the effect of pressure on the sphalerite–pyrite–pyrrhotite equilibrium

To calculate the molar volume of FeS and the partial molar volumes of FeS and ZnS in sphalerite, volumes were calculated in 5 mole percent intervals, from 0 to 55 mole percent FeS, from the expression in Barton and Toulmin (1966):

$$a_0 = 5.4093 + 0.0005637\ (\%\mathrm{FeS}) - 0.000004107\ (\%\mathrm{FeS})^2.$$

A polynomial was fitted to the volumes obtained at the twelve points to give:

$$\text{Volume (cm}^3) = 23.831 + 0.7452\ X^{sp}_{ZnS} - 0.5366\ X^{sp^2}_{FeS} - 0.006835\ X^{sp^3}_{FeS}$$

The volume equation was differentiated to obtain:

$$\frac{dV}{dX^{sp}_{FeS}} = 0.7452 - 1.0731\ X^{sp}_{FeS} - 0.02051\ X^{sp^2}_{FeS}.$$

This differential was evaluated at $X^{sp}_{FeS} = 0$ and $X^{sp}_{FeS} = 1$ to obtain the partial molar and excess partial molar volumes at infinite dilution, listed in Table 1. The polynomial for the volume was evaluated at $X^{sp}_{FeS} = 1$ to obtain the molar volume of FeS sphalerite. The relationship between molar volume, partial molar volume, excess partial molar volume, and composition is shown in Figure 4.

The excess partial molar volume at infinite dilution may be included in the $\bar{G}^{ex}$ term to allow the calculation of activity coefficients at any pressure, since:

$$\bar{G}^{ex}_{\infty} = \bar{U}^{ex}_{\infty} + P\bar{V}^{ex}_{\infty} \text{ and;}$$

$$\bar{G}^{ex}_{\infty ZnS} = 0.642\ T + 0.0131\ P \quad (4)$$

$$\bar{G}^{ex}_{\infty FeS} = 1.158\ T + 0.0130\ P \quad (5)$$

Using the molar volume of FeS pyrrhotite, obtained from the straight line fit by Froese and Gunter (1976) to the data of Fleet (1968), and the molar volume of FeS sphalerite (Table 1) at 25°C, ΔV_s for equilibrium (1) is:

$$V^{sp}_{FeS} - V^{po}_{FeS} = 24.033\ \text{cm}^3 - 18.198\ \text{cm}^3 = 5.835\ \text{cm}^3\ (0.1394\ \text{cal/bar}).$$

Table 1. Molar volumes, partial molar volumes, and excess partial molar volumes for ZnS and FeS at infinite dilution

	V^{sp}_{FeS}	V^{sp}_{ZnS}	$\bar{V}^{sp}_{\infty FeS}$	$\bar{V}^{sp}_{\infty ZnS}$	$\bar{V}^{sp\ ex}_{\infty FeS}$	$\bar{V}^{sp\ ex}_{\infty ZnS}$
cm^3	24.033	23.831	24.576	24.381	0.544	0.550
cal/bar	0.5741	0.5693	0.5871	0.5824	0.0130	0.0131

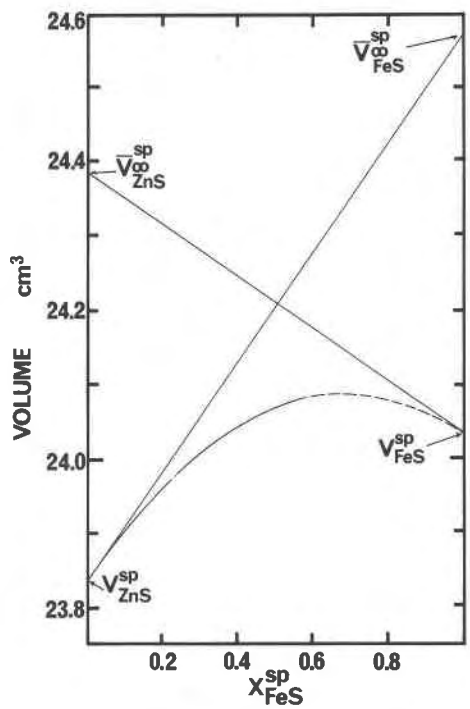

Fig. 4. Volume *vs.* composition of sphalerite, showing the relationship of molar volume (V^{sp}), partial molar volume at infinite dilution ($\bar{V}^{sp}_{\infty}$) and excess partial molar volume at infinite dilution ($\bar{V}^{sp}_{\infty} - V^{sp}$).

$\Delta G^0_{(1)}$ at any temperature is:

$$\Delta G^0_{(1)} = 239 - 0.840\ T \quad (6)$$

For a given pyrrhotite composition equilibrium (1) and the pyrite–pyrrhotite solvus from Toulmin and Barton (1964) can be used to obtain the composition of sphalerite coexisting with pyrite and pyrrhotite at any temperature and pressure.

First a^{po}_{FeS} on the pyrite–pyrrhotite solvus is calculated by a method similar to that of Froese and Gunter (1976). The solvus implies the equilibria:

$$\underset{\text{pyrrhotite}}{\text{FeS}} + \tfrac{1}{2}\,S_2 = \underset{\text{pyrite}}{\text{FeS}_2} \quad (7)$$

$$\underset{\text{(in pyrrhotite)}}{\square S} = \underset{\text{(in vapor)}}{\tfrac{1}{2}\,S_2} \quad (8)$$

At one atmosphere, fS_2 and a^{po}_{FeS} can be obtained from the expressions in Toulmin and Barton (1964), using the corresponding composition of pyrrhotite coexisting with pyrite. It is assumed that a^{po}_{FeS} is independent of pressure for any pyrrhotite composition. For equilibrium (7)

$$\Delta G^0_{(7)} = \tfrac{1}{2}\,RT \ln fS_2 + RT \ln a^{po}_{FeS} - \Delta V_s(P - 1) \quad (9)$$

and for equilibrium (8)

$$\Delta G^0_{(8)} = RT \ln a^{po}_{\square S} - \tfrac{1}{2} RT \ln fS_2 - \Delta V_s(P - 1) \quad (10)$$

From (9), $\Delta G^0_{(7)}$ can be calculated at any temperature for pyrrhotite compositions on the solvus and adjusted to any pressure using $\Delta V_s = 0.1372$ (Froese and Gunter, 1976), allowing the calculation of fS_2 at any pressure. For equilibrium (8) the term $\Delta G^0_{(8)} - RT \ln a^{po}_{\square S}$ can be treated as a constant equal to $-\frac{1}{2} RT \ln fS_2$, at one atmosphere. Assuming $a^{po}_{\square S}$ is independent of pressure and using $\Delta V_s = -0.3455$ cal/bar (Froese and Gunter, 1976), the equilibrium sulfur fugacity for (8) may be calculated at any pressure. Since equilibria (7) and (8) must apply simultaneously, the values of fS_2 must be equal, and a^{po}_{FeS} for the pyrite–pyrrhotite solvus can be calculated at higher pressures by selecting arbitrary pyrrhotite compositions and iterating for fS_2.

Now that a^{po}_{FeS} can be calculated at any pressure and temperature the composition of sphalerite coexisting with pyrite and pyrrhotite is obtained in the following manner.

The equilibrium constant for (1) is calculated at the desired pressure and temperature using $\Delta V_s = 0.1394$ cal/bar and the relationship $\Delta G^0 = -RT \ln K - \Delta V_s(P - 1)$. Knowing $K_{(1)}$ and a^{po}_{FeS} at the desired temperature and pressure, a^{sp}_{FeS} can be calculated from:

$$a^{sp}_{FeS} = K_{(1)} \cdot a^{po}_{FeS}$$

From (4) and (5) $\bar{G}^{ex}_{\infty FeS}$ and $\bar{G}^{ex}_{\infty ZnS}$ may be calculated and substituted into equation (2) to obtain γ^{sp}_{FeS}. Assuming arbitrary sphalerite compositions (X^{sp}_{FeS}), a second value for a^{sp}_{FeS} is obtained and X^{sp}_{FeS} may be iterated until both values of a^{sp}_{FeS} are equal. This provides the composition of sphalerite in equilibrium with pyrite and pyrrhotite. Calculations performed by Scott (1973) required estimated thermal expansion and compressibility data to obtain a calculated 5 kbar isobar which agreed with the experimental data. The isobars at 2.5, 5, and 7.5 kbars in Figure 5 were calculated without thermal expansion and compressibility and are in excellent agreement with the experimental brackets given by Scott (1973).

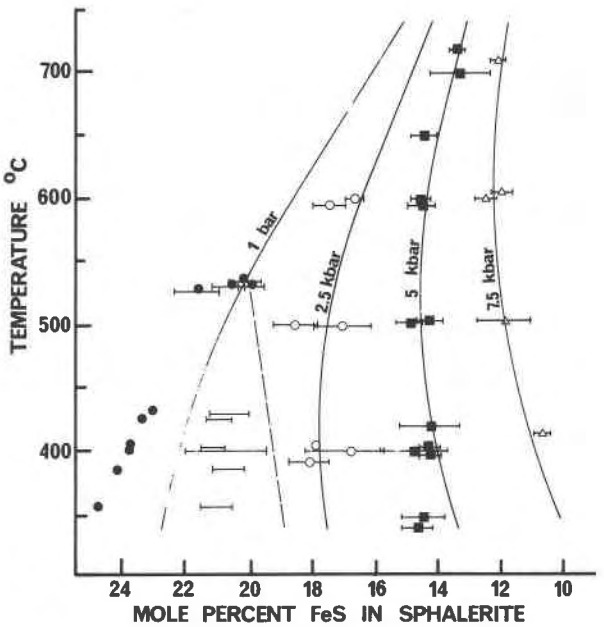

Fig. 5. Calculated isobars using the solution model and the pyrite–pyrrhotite equilibrium from Toulmin and Barton (1964) agree well with the experimental brackets from Scott (1973). The dashed 1 bar solvus isobar has been calculated assuming $a^{po}_{FeS} = 0.48$, as in Scott and Barnes (1971). Closed circles are the compositions of iron-rich patches in one-atmosphere experiments from Scott and Barnes (1971).

Fit of the solution model to experimental data

The solution model can be used with input values for a^{po}_{FeS} and temperature, at one bar, to predict the composition of sphalerite. Table 2 shows the compositions of sphalerite predicted by the solution model, compared with the experimentally measured compositions used to calculate the least-squares regression. Of the 113 points used, most predicted compositions are within approximately 2 mole percent FeS of the experimental composition, except 10 runs. No obvious reason can be found to exclude these runs, so they have been included in the final calculations. Table 3 shows the compositions of sphalerite predicted by the solution model for experimental runs not included in the regression. Run 42A (also excluded by Scott and Barnes, 1971) is anomalous, but the compositions of sphalerites in the 555°C runs, 60 C and 44E, are well described by the solution model.

The extrapolation of the solution model to lower temperatures can be tested by comparison with the data of Scott and Barnes (1971). The values of a^{po}_{FeS} and temperature from Scott and Barnes' Table 1 were used to predict sphalerite compositions coexisting with pyrrhotite. All runs except 320 (3 mole % FeS too low), 508, and 511 (excluded by Scott and Barnes) are within 2 mole percent FeS of the measured and pressure-adjusted sphalerite compositions in Scott and Barnes (1971, Table 1). The results are shown in Table 4.

The assemblage sphalerite–pyrite–pyrrhotite is of

Table 2. Fit of the solution model to the data of Barton and Toulmin (1966)

Run	T °C	a^{po}_{FeS}	Mole% FeS sphalerite input	calc.	diff.
28A	850	1.000	56.60	55.55	-1.05
29A	848	0.525	25.70	23.63	-2.07
30A	850	1.000	55.90	55.55	-0.35
31A	850	0.982	54.00	54.29	0.29
32A	850	0.956	53.00	52.47	-0.53
33A	850	0.898	48.50	48.40	-0.10
34A	850	0.824	43.10	43.22	0.12
35A	850	0.769	37.40	39.40	2.00
36A	850	0.696	33.70	34.45	0.75
37A	850	0.630	31.00	30.12	-0.88
38A	850	0.610	28.60	28.84	0.24
SL2	858	0.420	16.20	17.76	1.56
15A	847	0.761	38.90	38.84	-0.06
16A	847	0.810	43.30	42.23	-1.07
17A	847	0.852	47.40	45.16	-2.24
18A	847	0.948	51.20	51.89	0.69
19A	847	0.978	53.70	53.99	0.29
64A	850	0.940	46.00	51.35	5.35
65A	850	0.827	43.20	43.43	0.23
66A	850	0.751	38.30	38.17	-0.13
40A	848	1.000	55.90	55.53	-0.37
41A	848	0.941	51.90	51.41	-0.49
43A	848	0.623	30.50	29.66	-0.84
28B	790	1.000	55.80	55.13	-0.67
29B	780	0.508	21.60	22.43	0.83
30B	790	0.998	53.80	54.99	1.19
31B	790	0.982	52.80	53.88	1.08
32B	790	0.966	53.40	52.76	-0.64
33B	790	0.882	47.80	46.91	-0.89
34B	790	0.805	41.50	41.56	0.06
35B	790	0.765	40.40	38.81	-1.59
36B	790	0.701	33.00	34.50	1.50
37B	790	0.611	32.60	28.67	-3.93
38B	790	0.596	27.20	27.74	0.54
15B	801	0.752	37.30	37.99	0.69
16B	801	0.801	41.00	41.35	0.35
17B	801	0.849	44.70	44.68	-0.02
18B	801	0.950	50.50	51.73	1.23
19B	801	0.978	51.20	53.68	2.48
64B	780	0.939	50.50	50.81	0.31
65B	780	0.837	42.50	43.71	1.21
66B	780	0.710	33.20	35.05	1.85
42B	780	0.919	52.00	49.42	-2.58
43B	780	0.662	29.90	31.89	1.99
44B	780	0.555	24.70	25.19	0.49
28C	738	1.000	56.50	54.72	-1.78
29C	738	0.493	22.60	21.44	-1.16
30C	738	1.000	53.70	54.72	1.02
31C	738	0.980	55.80	53.34	-2.46
32C	738	0.948	52.10	51.13	-0.97
33C	738	0.873	47.30	45.93	-1.37
34C	738	0.819	44.10	42.20	-1.90
35C	738	0.782	39.30	39.66	0.36
36C	738	0.673	31.60	32.40	0.80
37C	738	0.586	27.20	26.91	-0.29
38C	738	0.531	25.60	23.62	-1.98
28D	704	1.000	54.70	54.44	-0.26
29D	704	0.476	20.40	20.38	-0.02
32D	704	0.955	48.00	51.34	3.34
33D	704	0.860	46.30	44.78	-1.52
34D	704	0.821	42.30	42.10	-0.20
35D	704	0.734	36.10	36.22	0.12
36D	704	0.669	31.50	31.96	0.46
37D	704	0.566	25.70	25.55	-0.15
38D	704	0.509	24.40	22.23	-2.17
G3	700	0.397	16.10	16.20	0.10
15D	700	0.742	35.40	36.73	1.33
16D	700	0.805	42.30	40.98	-1.32
17D	700	0.834	43.70	42.96	-0.74
18D	700	0.940	49.20	50.27	1.07
19D	700	0.967	54.50	52.13	-2.37
20D	700	0.397	17.90	16.20	-1.70
64C	700	0.924	44.00	49.17	5.17
66C	700	0.709	32.60	34.54	1.94
42C	700	0.855	45.30	44.41	-0.89
43C	700	0.605	27.60	27.90	0.30
44C	700	0.475	21.30	20.32	-0.98
28E	640	1.000	52.70	53.85	1.15
29E	640	0.441	17.90	18.29	0.39
30E	640	1.000	52.70	53.85	1.15
31E	640	0.975	51.60	52.14	0.54
32E	640	0.954	50.10	50.70	0.60
33E	640	0.867	45.20	44.75	-0.45
34E	640	0.811	41.60	40.94	-0.66
35E	640	0.758	34.50	37.39	2.89
36E	640	0.662	31.10	31.14	0.04
37E	640	0.545	25.80	24.03	-1.77
38E	640	0.479	21.60	20.32	-1.28
G6	650	0.428	17.30	17.64	0.34
P31	636	0.434	18.60	17.91	-0.69
15E	636	0.716	34.70	34.59	-0.11
16E	636	0.758	38.90	37.36	-1.54
17E	636	0.793	45.30	39.70	-5.60
18E	636	0.945	49.20	50.05	0.85
19E	636	0.967	48.00	51.55	3.55
20E	636	0.434	18.10	17.91	-0.19
G11	600	0.455	18.30	18.88	0.58
15F	600	0.725	31.60	34.92	3.32
16F	600	0.781	38.90	38.61	-0.29
17F	600	0.826	40.20	41.62	1.42
18F	600	0.934	45.70	48.95	3.25
19F	600	0.969	49.20	51.33	2.13
20F	600	0.455	16.80	18.88	2.08
28F	580	1.000	52.10	53.22	1.12
31F	580	0.983	51.50	52.07	0.57
32F	580	0.951	52.00	49.90	-2.10
33F	580	0.850	45.70	43.05	-2.65
34F	580	0.784	42.00	38.64	-3.36
35F	580	0.730	34.10	35.09	0.99
36F	580	0.629	29.60	28.72	-0.88
37F	580	0.527	22.10	22.72	0.62
38F	580	0.460	20.80	19.07	-1.73
60B	580	0.460	17.80	19.07	1.27

primary interest and the high-pressure experimental data of Scott are reproduced by the calculated isobars in Figure 5. The calculated 1 bar curve lies between the composition of the matrix and iron-rich patches in Scott and Barnes' (1971, Figures 7 and 9, Table 2) experiments at temperatures below 525°C. Table 5 and the dashed curve in Figure 5 show the fit of the solution model to the matrix compositions in sphalerite–pyrite–pyrrhotite assemblages if a^{po}_{FeS} = 0.48 is assumed constant below 525°C as in Scott and Barnes. They obtain a^{po}_{FeS} by plotting matrix sphalerite compositions and a curve fitted to the data of Barton and Toulmin (1966) over a temperature range from 1104 to 550°C, on a graph of a^{po}_{FeS} *vs.* mole percent FeS in sphalerite. The fitted curve was then extrapolated to approx. 20 mole percent FeS (see Figure 1, Scott and Barnes, 1971) to obtain a^{po}_{FeS} = 0.48 and constant below 525°C because of the constant matrix compositions. Craig and Scott (1974) state that the experiments of Schneeberg (1973) confirm their choice of the pyrite–pyrrhotite equilibrium. Figure 6 shows the data of Schneeberg, compared with the data of Toulmin and Barton (1964, Table 5) and the curve drawn by Scott and Barnes. At 500°C, $\log f S_2$ from Scott and Barnes and Toulmin and Barton are similar. At 325°C, $\log f S_2$ from Toulmin and Barton is 0.3 $\log f S_2$ lower than $\log f S_2$ from Scott and Barnes, but the difference is within the 0.35 $\log f S_2$ error estimated by Toulmin and Barton. This minor variation in $\log f S_2$ is responsible for the discrepancy between a^{po}_{FeS} = 0.48 (Scott and Barnes) and a^{po}_{FeS} = 0.55 (Toulmin and Barton) at 325°C. It is apparent that very small variations in the pyrite–pyrrhotite equilibrium can cause large changes in the equilibrium FeS content of sphalerite.

Table 3. Fit of the data from Barton and Toulmin (1966, Table 3) not used to calculate the sphalerite solution model

Run	T °C	a^{po}_{FeS}	Mole% FeS sphalerite input	calc.	diff.
33L	1104	0.907	49.80	50.31	0.51
35L	1104	0.794	39.80	42.23	2.43
36L	1104	0.764	38.50	40.11	1.61
28L	1000	1.000	56.60	56.43	-0.17
31L	1000	0.990	54.20	55.73	1.53
32L	1001	0.946	54.10	52.62	-1.48
34L	1001	0.827	42.20	44.17	1.97
28J	925	1.000	58.10	56.01	-2.09
35J	925	0.776	39.80	40.25	0.45
36J	925	0.729	36.80	37.00	0.20
37J	925	0.665	31.10	32.69	1.59
42A	848	0.806	54.60	41.95	-12.65
600	555	0.472	19.00	19.60	0.60
44E	555	0.472	19.70	19.60	-0.10

Table 4. Fit of the sphalerite solution model to the low-temperature data of Scott and Barnes (1971, Table 2) for experiments in which sphalerite and pyrrhotite coexist

Run	T °C	a^{po}_{FeS}	Mole% FeS sphalerite input	calc.	diff.
311	487	0.678	32.00	31.03	-0.97
312	487	0.705	33.60	32.71	-0.89
320	396	0.767	38.60	35.60	-3.00
326	445	0.675	30.10	30.47	-0.37
327	524	0.600	26.70	26.61	-0.09
331	581	0.634	27.50	29.03	-1.53
351	431	0.604	27.40	26.14	-1.26
352	427	0.670	31.00	29.99	-1.01
505	408	0.824	39.70	39.38	-0.32
508	331	0.801	46.20	36.77	-9.43
511	331	0.810	45.90	37.33	-8.57
515	351	0.685	31.70	30.04	-1.66

Pressure during metamorphism at the Stall Lake mine

From the intersection of the kyanite–sillimanite transition, calculated from the data of Richardson *et al.* (1968), and the equilibrium:

chlorite + muscovite = biotite + staurolite + quartz + H_2O

from Hoschek (1969), Froese and Gasparrini (1975) estimate the pressure of metamorphism at Stall Lake, in the Snow Lake area, to be approximately 5.5 kbar. Using the aluminosilicate data from Holdaway (1971) would give a pressure of 6 kbar. Figure 7 shows calculated isobars from this study, isobars drawn by Scott from experimental brackets, and sphalerite compositions from pyrite–pyrrhotite bearing rocks reported by Bristol (1974). From these data the total metamorphic pressure is 7 ± 0.9 kbar using Scott's isobars, and 7 ± 1 kbar from the isobars calculated in this study. The pressures estimated using the calibration of Scott (1973) or the calculations

Table 5. Fit of data from Scott and Barnes (1971, Table 2) for the equilibrium among sphalerite–pyrite–pyrrhotite at one bar, using matrix compositions and a constant activity of FeS in pyrrhotite = 0.48 below 525°C

Run	T °C	a^{po}_{FeS}	Mole% FeS sphalerite input	calc.	diff.
348	534	0.480	20.10	19.93	-0.17
349	527	0.480	21.60	19.90	-1.70
353	425	0.480	20.90	19.34	-1.56
354	428	0.480	20.60	19.36	-1.24
361	529	0.480	20.60	19.91	-0.69
362	529	0.480	19.90	19.91	0.01
364	384	0.480	20.60	19.08	-1.52
513	354	0.480	21.00	18.87	-2.13
521	402	0.480	21.10	19.20	-1.90
526	399	0.480	20.70	19.16	-1.52

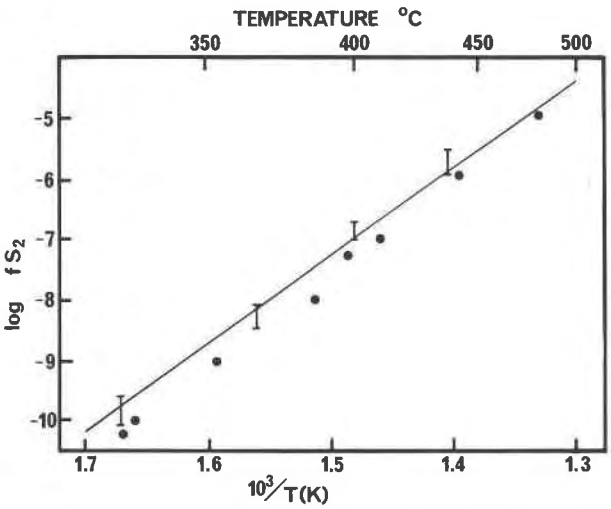

Fig. 6. A plot of log fS_2 *vs.* temperature shows that a small change in log fS_2 of approximately 0.3 log units will account for the difference, at 350°C, in a^{po}_{FeS} = 0.48 from Scott and Barnes (1971, shown by the solid curve and calculated using the matrix compositions of sphalerite, and a^{po}_{FeS} = 0.55, as a function of temperature from Table 5 (solid circles) of Toulmin and Barton (1964). The vertical bars are the experimental work of Schneeberg (1973).

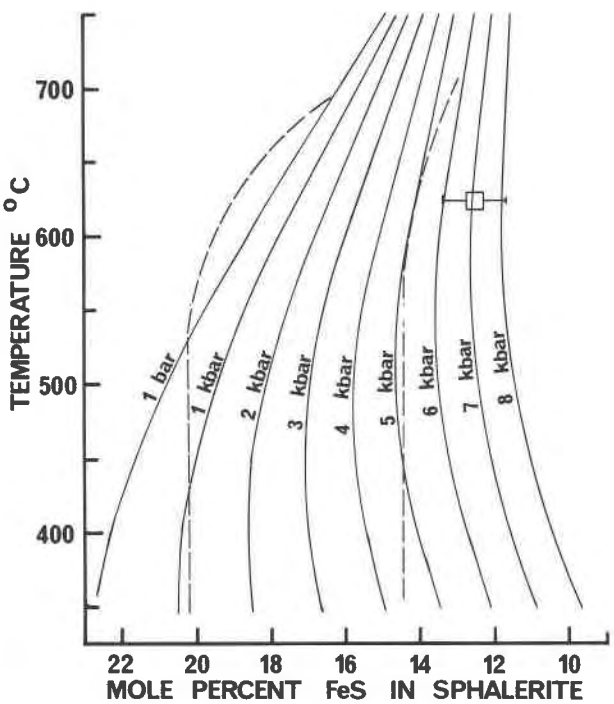

Fig. 7. Calculated isobars from this study (solid curves) are comparable to the experimentally determined isobars from Scott (1973), shown by the dashed curves. The open square with the bar represents the range of compositions of sphalerite coexisting with pyrite and pyrrhotite reported by Bristol (1974) from the Stall Lake mine near Snow Lake, Manitoba.

in this study are slightly higher than pressures estimated from pelitic assemblages.

Conclusions

A Margules (sub-regular) solution model can be applied to the data of Barton and Toulmin (1966) and used with measured and estimated thermodynamic properties and the pyrite–pyrrhotite equilibrium to calculate the *P–T–X* phase relations of the assemblage sphalerite–pyrite–pyrrhotite. The solution model, based on data from 850 to 580°C, can be extrapolated to higher and lower temperatures and adequately predicts sphalerite compositions at lower temperatures from the experiments of Scott and Barnes (1971). For sphalerite–pyrite–pyrrhotite, the shape of the 1 bar solvus is dependent on the pyrite–pyrrhotite solvus data used in the calculations. If a^{po}_{FeS} is kept constant at 0.48 below 550°C, as in Scott and Barnes, the solution model will predict sphalerite compositions approximately the same as the matrix compositions for sphalerite in Scott and Barnes (1971, Table 2). If a^{po}_{FeS} is allowed to vary with temperature below 550°C (*i.e.* calculated from Toulmin and Barton), then the solution model predicts sphalerite compositions between the compositions of the iron-rich patches and the matrix compositions from Scott and Barnes (1971). Both assumptions are consistent with the data of Barton and Toulmin (1966) or the data above 500°C from Scott and Barnes (1971). Isobars calculated for higher pressures, based on values of a^{po}_{FeS} as calculated from Toulmin and Barton (1964), are in agreement with experimental work at higher pressures from Scott (1973).

The calculated isobars can be applied to sphalerite compositions from Stall Lake, Manitoba, and predict pressures in general agreement with pressures estimated from pelitic assemblages by Froese and Gasparrini (1975) and pressures estimated from the sphalerite geobarometer by Scott (1976).

Acknowledgments

I am indebted to Edgar Froese for suggesting an examination of the thermodynamic properties of sphalerite, suggestions in the calculations, and critical readings of the manuscript. A critical review by S.D. Scott suggested ideas for improvements of the final calculations. This work forms part of a Ph.D. thesis at Carleton University, and I am grateful for help from Cathy Chan with statistics, and the guidance and support of my adviser, George Skippen and NRC grant A4253 to him.

References

Barton, P. B. Jr. and P. Toulmin III (1966) Phase relations involving sphalerite in the Fe–Zn–S system. *Econ. Geol., 61,* 815–849.

Boorman, R. S. (1967) Subsolidus studies in the ZnS–FeS–FeS_2 system. *Econ. Geol., 62,* 614–631.

Bristol, C. C. (1974) Sphalerite geobarometry of some metamorphosed orebodies in the Flin Flon and Snow Lake districts, Manitoba. *Can. Mineral., 12,* 308–315.

Carlson, H. C. and A. P. Colburn (1942) Vapor-liquid equilibrium of nonideal solutions. *Ind. Eng. Chem., 34,* 581–589.

Craig, J. R. and S. D. Scott (1974) Sulfide phase equilibria. In P. H. Ribbe, Ed., *Sulfide Mineralogy,* Vol. 1, *Mineral. Soc. Am. Short Course Notes.*

Denbigh, K. (1971) *The Principles of Chemical Equilibrium.* Cambridge University Press, London.

Einaudi, M. T. (1968) Sphalerite–pyrrhotite–pyrite equilibria—a re-evaluation. *Econ. Geol., 63,* 832–834.

Fleet, M. E. (1968) On the lattice parameters and superstructures of pyrrhotites. *Am. Mineral., 53,* 1846–1855.

——— (1975) Thermodynamic properties of (Zn,Fe)S solid solutions at 850°C. *Am. Mineral., 60,* 466–470.

Froese, E. and E. Gasparrini (1975) Metamorphic zones in the Snow Lake area, Manitoba. *Can. Mineral., 13,* 162–167.

——— and A. Gunter (1976) A note on the pyrrhotite-sulfur vapor equilibrium. *Econ. Geol., 71,* 1589–1594.

Holdaway, M. J. (1971) Stability of andalusite and the aluminum silicate phase diagram. *Am. J. Sci., 271,* 97–131.

Hoschek, G. (1969) The stability of staurolite and chloritoid and their significance in the metamorphism of pelitic rocks. *Contrib. Mineral. Petrol., 22,* 208–232.

Kullerud, G. (1953) The FeS–ZnS system, a geological thermometer. *Norsk Geol. Tidsskr., 32,* 61–147.

Lusk, J., F. A. Campbell and H. R. Krouse (1975) Application of sphalerite geobarometry and sulfur isotope geothermometry to ores of the Quemont Mine, Noranda, Quebec. *Econ. Geol., 70,* 1070–1083.

Margules, M. (1895) Uber die Zusammensetzung der gesattigten Dampfe von Mischungen. *Sitzungsber. Akad. Wiss. Wien, 104,* 1243–1278.

Richardson, S. W., P. M. Bell and M. C. Gilbert (1968) Kyanite–sillimanite equilibrium between 700° and 1500°C. *Am. J. Sci., 266,* 513–541.

Schneeberg, E. P. (1973) Sulfur fugacity measurements with the electrochemical cell Ag| AgI| $Ag_{2+x}S$,fS_2. *Econ. Geol., 68,* 507–517.

Scott, S. D. (1973) Experimental calibration of the sphalerite geobarometer. *Econ. Geol., 68,* 466–474.

——— (1976) Application of the sphalerite geobarometer to regionally metamorphosed terrains. *Am. Mineral., 61,* 661–670.

——— and H. L. Barnes (1971) Sphalerite geothermometry and geobarometry. *Econ. Geol., 66,* 653–669.

Toulmin, P. III and P. B. Barton Jr. (1964) A thermodynamic study of pyrite and pyrrhotite. *Geochim. Cosmochim. Acta, 28,* 641–671.

Manuscript received, February 4, 1977; accepted for publication, August 30, 1977.